

Supporting Information

Investigation of easy-plane magnetic anisotropy in P-ligand square-pyramidal Co^{II} single ion magnets

Amit Kumar Mondal,^a Jesús Jover,^b Eliseo Ruiz*^b and Sanjit Konar*^a

^a *Department of Chemistry, IISER Bhopal, Bhopal By-Pass Road, Bhauri, Bhopal 462066, M. P., India.*

^b *Departament de Química Inorgànica and Institut de Recerca de Química Teòrica i Computacional, Universitat de Barcelona, Diagonal 645, E-08028 Barcelona, Spain.*

X-ray Crystallography. Intensity data were collected on a Brüker APEX-II CCD diffractometer using a graphite monochromated Mo-K α radiation ($\alpha = 0.71073 \text{ \AA}$) at 296 K. Data collection was performed using φ and ω scan. The structure was solved using direct methods followed by full matrix least square refinements against F^2 (all data HKLF 4 format) using SHELXTL.¹ Subsequent difference Fourier synthesis and least-square refinement revealed the positions of the remaining non-hydrogen atoms. Determinations of the crystal system, orientation matrix, and cell dimensions were performed according to the established procedures. Lorentz polarization and multi-scan absorption correction was applied. Non-hydrogen atoms were refined with independent anisotropic displacement parameters and hydrogen atoms were placed geometrically and refined using the riding model. All calculations were carried out using SHELXL 97,² PLATON 99,³ and WinGX systemVer-1.64.⁴ Crystallographic data for complex **1** and **2** were summarized in Table S1.

Synthesis of ligand PP₃: Diphenylphosphine (11.8 g, 62.9 mmol) was added to a suspension of potassium *tert*-butoxide (18.1 g, 160.9 mmol) in dry and freshly distilled THF (200 ml) under argon. The resulting deep red solution was stirred for 30 min and tris(2-chloroethyl)phosphine hydrochloride (5.3 g, 20.8 mmol) was added to the above solution. The mixture was refluxed for 20 h at 80°C, poured into 500 ml of water and cooled in an ice bath. The ligand precipitated and was filtered off, recrystallized from DMF/H₂O and washed with EtOH. Yield: 81 %, mp 102°C. Anal. Calcd. for C₄₂H₄₂P₄: C, 75.22; H, 6.31 %. Found: C, 75.34; H, 6.40 %.

Synthesis of complex 1: Ligand PP₃ (67 mg, 0.1 mmol) was dissolved in MeCN (5 ml) and the solution was warmed to 50°C. The mixture of CoCl₂·6H₂O (12 mg, 0.05 mmol) and Co(ClO₄)₂·6H₂O (18 mg, 0.05 mmol) dissolved in MeOH (5 ml) was added dropwise to the above ligand solution while stirring. The resulting solution forms an intense blue mixture that was stirred overnight at room temperature. The solution was then filtered off and the filtrate was left at open atmosphere for slow evaporation which yields large X-ray quality crystals of [Co(PP₃)Cl]·ClO₄ (**1**) after 4 days. The crystals were separated, washed with cold water and Et₂O and air-dried yield (76 %). Anal. Calcd. for C₄₂H₄₂CoP₄O₄Cl₂: C, 58.35; H, 4.90 %. Found: C, 58.45; H, 4.97 %. IR (KBr pellet, 4000 – 400 cm⁻¹) ν /cm⁻¹: 3064, 2976, 1582, 1460, 1419, 1371, 743, 622.

Synthesis of complex 2: Ligand PP₃ (67 mg, 0.1 mmol) was dissolved in MeCN (5 ml) and the solution was warmed to 50°C. The mixture of CoBr₂ (11 mg, 0.05 mmol) and Co(ClO₄)₂·6H₂O (18 mg, 0.05 mmol) dissolved in MeOH (5 ml) was added dropwise to the above ligand solution while stirring. The resulting

solution forms an intense blue mixture that was stirred overnight at room temperature. The solution was then filtered off and the filtrate was left at open atmosphere for slow evaporation which yields large X-ray quality crystals of $[\text{Co}(\text{PP}_3)\text{Br}]\cdot\text{ClO}_4$ (**2**) after 3 days. The crystals were separated, washed with cold water and Et_2O and air-dried yield (68 %). Anal. Calcd for $\text{C}_{42}\text{H}_{42}\text{CoP}_4\text{O}_4\text{ClBr}$: C, 55.50; H, 4.66 %. Found: C, 55.59; H, 4.58 %. IR (KBr pellet, 4000 – 400 cm^{-1}) ν / cm^{-1} : 3061, 2978, 1578, 1462, 1414, 1365, 747, 620.

Physical Measurements. Magnetic measurements were performed using a Quantum Design SQUID-VSM magnetometer. The measured values were corrected for the experimentally measured contribution of the sample holder, while the derived susceptibilities were corrected for the diamagnetic contribution of the sample, estimated from Pascal's tables.⁵ Elemental analysis was performed on Elementar Microvario Cube Elemental Analyzer. IR spectrum was recorded on KBr pellets with a Perkin-Elmer spectrometer. Powder X-ray diffraction (PXRD) data was collected on a PANalytical EMPYREAN instrument using Cu-K α radiation.

Computational Details. The calculation of the second-order magnetic anisotropy (or zero-field splitting) parameters (D and E) has been carried out with two different software packages: MOLCAS⁶ and ORCA.⁷ We have employed MOLCAS (along with the SINGLE_ANISO⁸ code) to carry out a CASSCF calculation of the energy states of the Co^{II} complex. After that, the spin-orbit coupling has been introduced, as implemented in the SO-RASSI (Restricted Active Space State Interaction) approach, to mix up these energies and obtaining the final energy states. In these calculations we have employed an all electron ANO-RCC basis set:⁹ Co atoms (6s5p4d2f), P (5s4p3d2f), Cl 5s4p3d2f, C (3s2p) and H (2s).

A similar CASSCF calculation was carried out with ORCA; in this case the spin-orbit effects were included using the quasi-degenerate perturbation theory (QDPT). In these calculations all the atoms are described by the def2-TZVPP basis set,¹⁰ including the corresponding auxiliary basis sets for correlation and Coulomb fitting.

In both sets of calculations, the active space is formed by the seven d electrons of the Co^{II} centers and the 5d orbitals (7,5); and all the quadruplet (10) and doublet (40) states have been taken into account.

Further PT2 calculations were carried out with ORCA (NEVPT2) and MOLCAS (CASPT2) but they were not able to provide useful insights. The NEVPT2 calculations produced $\frac{1}{2}$ ground states, probably due to problems handling the active space orbitals. On the other hand, the CASPT2 calculations from MOLCAS showed serious convergence problems and were thus finally discarded.

Table S1. X-ray Crystallographic Data and Refinement Parameters for complex **1** and **2**.

| | 1 | 2 |
|-----------------------------------------------|---------------------------------------------------------------------------------|----------------------------------------------------------------------|
| Formula | C ₄₂ H ₄₂ CoP ₄ O ₄ Cl ₂ | C ₄₂ H ₄₂ CoP ₄ O ₄ ClBr |
| M _w (g mol ⁻¹) | 864.47 | 908.92 |
| Crystal size (mm) | 0.45×0.15×0.10 | 0.48×0.20×0.18 |
| Crystal system | Triclinic | Triclinic |
| Space group | <i>P</i> -1 | <i>P</i> -1 |
| T (K) | 120(2) | 110(2) |
| a (Å) | 12.0627(17) | 12.0455(8) |
| b (Å) | 12.1504(17) | 12.1848(8) |
| c (Å) | 16.106(2) | 16.0981(9) |
| α (°) | 70.858(5) | 71.615(2) |
| β (°) | 88.701(6) | 89.089(3) |
| γ (°) | 63.249(5) | 63.295(2) |
| V (Å ³) | 1969.4(5) | 1980.8(2) |
| Z | 2 | 2 |
| ρ _{calcd} (g cm ⁻³) | 1.458 | 1.524 |
| μ(MoKα) (mm ⁻¹) | 0.776 | 1.713 |
| <i>F</i> (000) | 894.0 | 930.0 |
| T _{max} , T _{min} | 0.915, 0.880 | 0.725, 0.680 |
| h, k, l range | -16 ≤ <i>h</i> ≤ 16, -16 ≤ <i>k</i> ≤ 16, -21 ≤ <i>l</i> ≤ 21 | -14 ≤ <i>h</i> ≤ 14, -14 ≤ <i>k</i> ≤ 14, -19 ≤ <i>l</i> ≤ 19 |
| Collected reflections | 10207 | 7038 |
| Independent reflections | 8324 | 6402 |
| Goodness-of-fit (GOF) on F ² | 1.003 | 1.159 |
| R1, wR2 (<i>I</i> > 2σ _{<i>I</i>}) | 0.0325, 0.0721 | 0.0237, 0.0718 |
| R1, wR2 (all data) | 0.0485, 0.0788 | 0.0290, 0.0863 |
| CCDC Number | 1455159 | 1455160 |

$R1 = \frac{\sum ||F_o| - |F_c||}{\sum |F_o|}$ and $wR2 = \frac{|\sum w(|F_o|^2 - |F_c|^2)|}{\sum w(F_o)^2}^{1/2}$

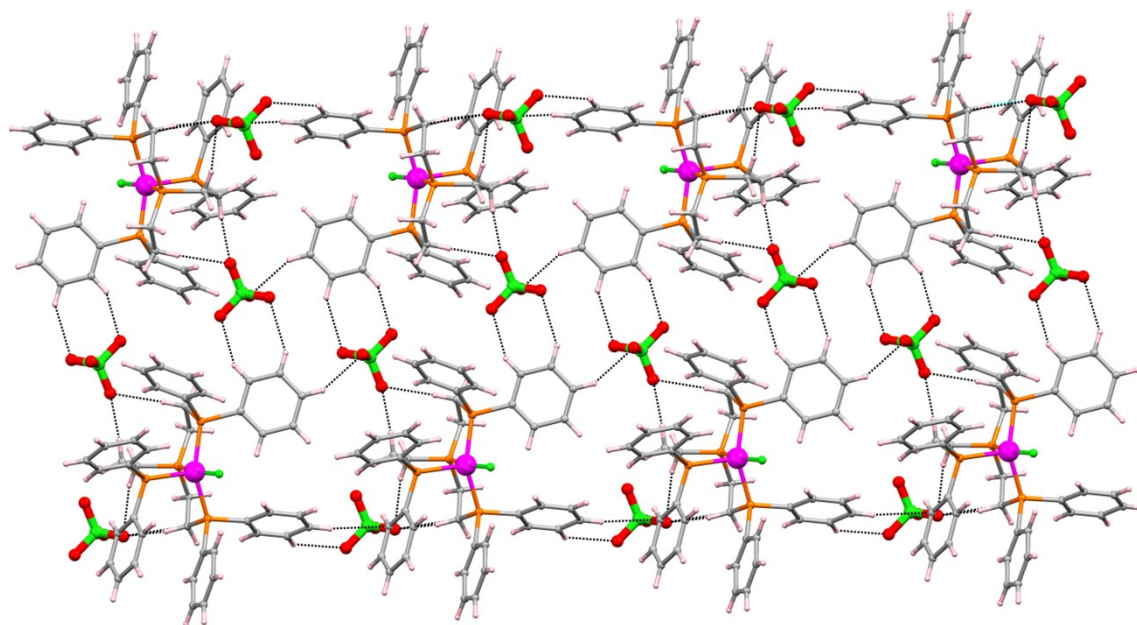
Table S2. Bond distances (Å) and bond angles (°) around Co^{II} centers found in complex **1** and **2**.

| Bond distance (Å) | | | | | |
|-------------------|------------|-----------|------------------|------------|------------|
| Complex 1 | Co1—P1 | 2.2501(3) | Complex 2 | Co1—P1 | 2.2459(3) |
| | Co1—P2 | 2.2702(2) | | Co1—P2 | 2.1562(5) |
| | Co1—P3 | 2.2816(3) | | Co1—P3 | 2.2797(5) |
| | Co1—P4 | 2.1558(1) | | Co1—P4 | 2.2733(5) |
| | Co1—Cl1 | 2.2482(1) | | Co1—Br1 | 2.3831(1) |
| Bond angle (°) | | | | | |
| Complex 1 | P2—Co1—P1 | 149.81(7) | Complex 2 | P3—Co1—P1 | 149.60(15) |
| | P2—Co1—P4 | 84.55(8) | | P3—Co1—P4 | 102.48(15) |
| | P2—Co1—P3 | 102.06(8) | | P3—Co1—P2 | 84.37(16) |
| | P1—Co1—P4 | 83.91(8) | | P1—Co1—P4 | 104.97(16) |
| | P1—Co1—P3 | 105.12(8) | | P1—Co1—P2 | 84.07(16) |
| | P4—Co1—P3 | 87.21(8) | | P4—Co1—P2 | 87.38(15) |
| | Cl1—Co1—P2 | 96.39(8) | | Br1—Co1—P3 | 96.96(13) |
| | Cl1—Co1—P1 | 90.34(8) | | Br1—Co1—P1 | 90.40(13) |
| | Cl1—Co1—P4 | 169.71(7) | | Br1—Co1—P4 | 101.09(13) |
| | Cl1—Co1—P3 | 102.56(7) | | Br1—Co1—P2 | 170.87(13) |

Table S3: Summary of SHAPE analysis for complexes **1-2**.

| | | | |
|---------|---|-----------------|--------------------------------|
| PP-5 | 1 | D _{5h} | Pentagon |
| vOC-5 | 2 | C _{4v} | Vacant octahedron |
| TBPY-5 | 3 | D _{3h} | Trigonal bipyramid |
| SPY-5 | 4 | C _{4v} | Spherical square pyramid |
| JTBPY-5 | 5 | D _{3h} | Johnson trigonal bipyramid J12 |

| Structure [ML ₅] | PP-5 | vOC-5 | TBPY-5 | SPY-5 | JTBPY-5 |
|------------------------------|--------|-------|--------|--------------|---------|
| Complex 1 | 31.733 | 1.813 | 3.313 | 1.136 | 6.214 |
| Complex 2 | 32.160 | 1.898 | 3.290 | 1.407 | 5.691 |

**Fig. S1.** A view of supramolecular 2D arrangement of complex **1** through intermolecular H-bonding and CH \cdots π interactions.

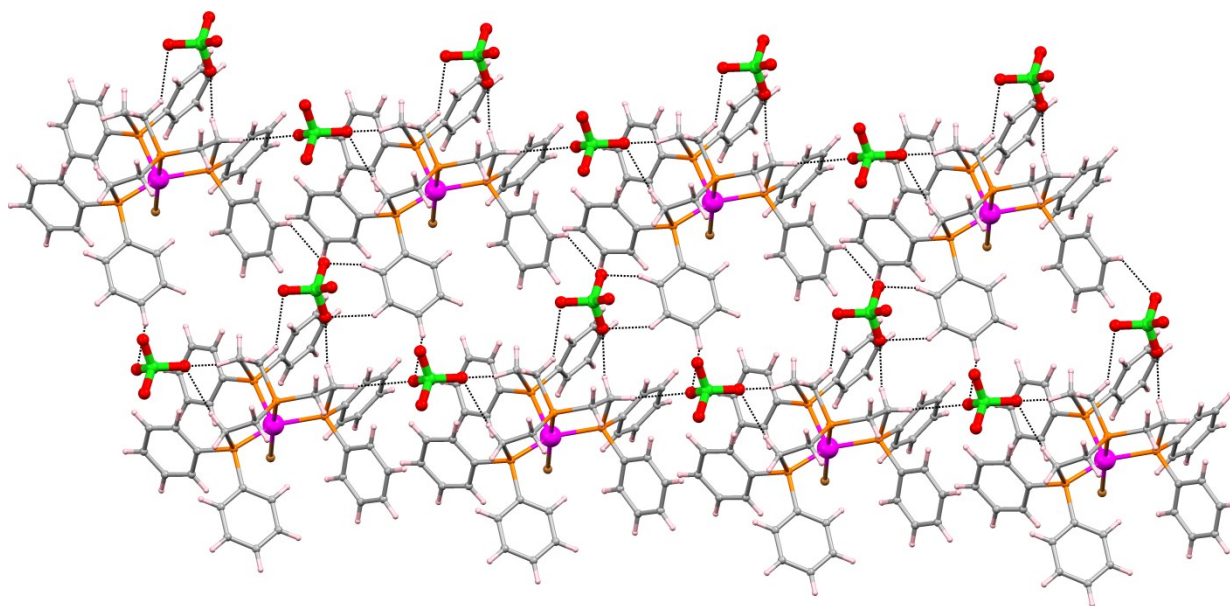


Fig. S2. A view of supramolecular 2D arrangement of complex **2** through intermolecular H-bonding and CH $\cdots\pi$ interactions.

Table S4. H-bond parameters found in complex **1**.

| D-H \cdots A | D-H(\AA) | H \cdots A(\AA) | D \cdots A (\AA) | \angle D-H-A($^\circ$) | Symmetry [#] |
|----------------------|---------------------|------------------------------|-------------------------------|----------------------------|-----------------------|
| C8-H8 \cdots C11 | 0.950 | 2.78 | 3.575(2) | 142 | 0 |
| C20-H20 \cdots C11 | 0.950 | 2.62 | 3.467(2) | 148 | 0 |
| C26-H26 \cdots C11 | 0.950 | 2.76 | 3.581(2) | 145 | 0 |
| C7-H7 \cdots C11 | 0.950 | 2.74 | 3.580(2) | 147 | 1 |
| C35-H35 \cdots O3 | 0.950 | 2.49 | 3.336(3) | 148 | 2 |
| C38-H38A \cdots O3 | 0.990 | 2.57 | 3.540(3) | 168 | 3 |
| C38-H38B \cdots O2 | 0.990 | 2.48 | 3.196(3) | 129 | 4 |
| C41-H41B \cdots O2 | 0.990 | 2.58 | 3.547(3) | 167 | 4 |
| C40-H40A \cdots O4 | 0.990 | 2.45 | 3.404(3) | 162 | 5 |

(0) x,y,z; (1) 1-x,2-y,-z; (2) -x,1-y,1-z; (3) 1-x,-y,1-z; (4) 1+x,y,z; (5) 1-x,1-y,1-z.

Table S5. H-bond parameters found in complex **2**.

| D-H \cdots A | D-H(\AA) | H \cdots A(\AA) | D \cdots A (\AA) | \angle D-H-A($^\circ$) | Symmetry [#] |
|----------------------|---------------------|------------------------------|-------------------------------|----------------------------|-----------------------|
| C3-H3 \cdots Br1 | 0.950 | 2.88 | 3.649(4) | 138 | 0 |
| C13-H13 \cdots Br1 | 0.950 | 2.73 | 3.566(3) | 147 | 0 |
| C21-H21 \cdots Br1 | 0.950 | 2.87 | 3.703(3) | 147 | 0 |
| C2-H2 \cdots Br1 | 0.950 | 2.85 | 3.736(3) | 156 | 1 |
| C29-H29 \cdots O3 | 0.950 | 2.51 | 3.354(4) | 148 | 2 |
| C37-H37A \cdots O1 | 0.990 | 2.44 | 3.397(4) | 162 | 3 |
| C41-H42B \cdots O1 | 0.990 | 2.59 | 3.368(3) | 135 | 3 |
| C40-H40A \cdots O3 | 0.990 | 2.59 | 3.559(3) | 167 | 4 |
| C40-H40B \cdots O4 | 0.990 | 2.45 | 3.181(4) | 168 | 5 |
| C41-H41B \cdots O4 | 0.990 | 2.56 | 3.539(3) | 135 | 5 |

(0) x,y,z; (1) 1-x,2-y,-z; (2) -x,1-y,1-z; (3) 1-x,1-y,1-z; (4) 1-x,-y,1-z; (5) 1+x,y,z.

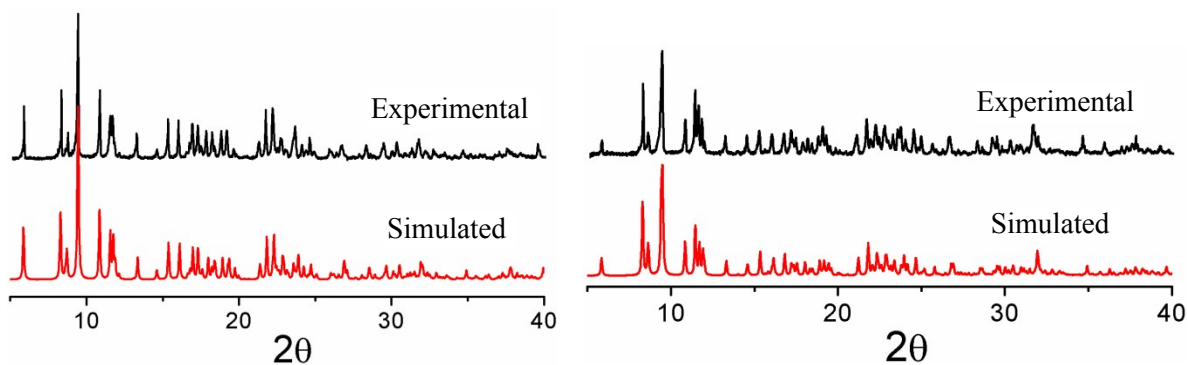


Fig. S3. PXRD patterns of complex 1 (left) and 2 (right).

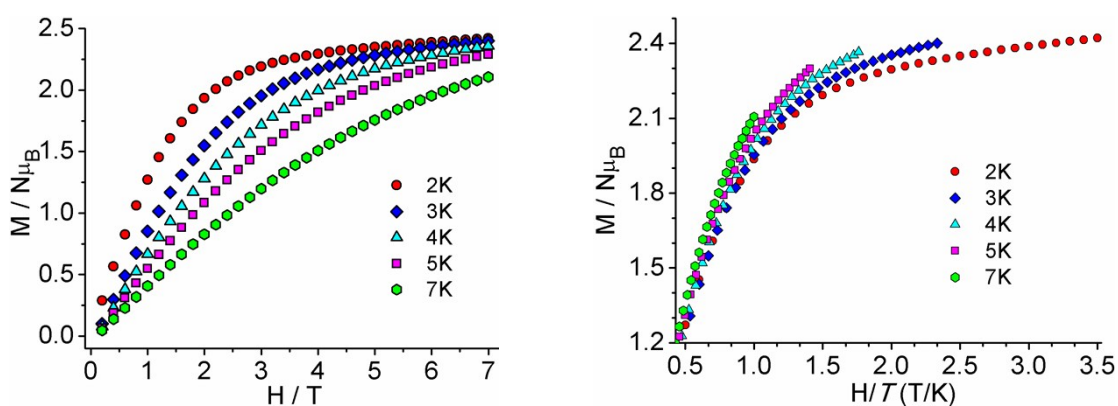


Fig. S4. $M/N\mu_B$ vs. H plots for complex 1 at the indicated temperatures (left); Plots of $M/N\mu_B$ vs. H/T for complex 1 at the indicated temperatures (right).

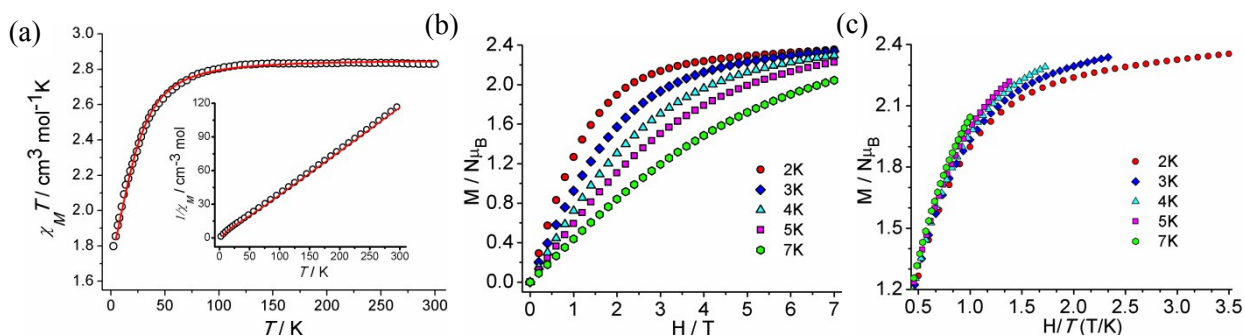


Fig. S5. $\chi_M T$ vs. T plots measured at 0.1 T for complex 2 (a); $1/\chi_M$ vs. T plot shown in the inset. The red lines are the best fit.; $M/N\mu_B$ vs. H plots for complex 2 at the indicated temperatures (b); Plots of $M/N\mu_B$ vs. H/T for complex 2 at the indicated temperatures (c).

Table S6. ORCA CASSCF computed spin-free and spin-orbit state energies for complex **1**.

| Spin-free energies (cm ⁻¹) | Spin-orbit states (cm ⁻¹) | CASSCF computed results | | | | | |
|----------------------------------------|---------------------------------------|------------------------------------------------|---------|----------------|----------|----------|----------|
| | | | | | | | |
| 0.0 | 0.0 | g _X | 2.025 | X _M | -0.92681 | -0.01102 | -0.37537 |
| 1568.7 | 86.6 | g _Y | 2.272 | Y _M | 0.02319 | -0.99934 | -0.02793 |
| 3002.7 | 1677.0 | g _Z | 2.554 | Z _M | -0.37482 | -0.03459 | 0.92645 |
| 3993.4 | 1775.4 | | | | | | |
| 6647.6 | 3007.7 | D _X | 7.718 | X _A | -0.96973 | -0.00576 | -0.24410 |
| 10242.2 | 3175.3 | D _Y | -11.320 | Y _A | 0.01226 | -0.99961 | -0.02515 |
| 10895.8 | 4337.8 | D _Z | 38.258 | Z _A | -0.24386 | -0.02738 | 0.96943 |
| 11923.8 | 6792.5 | D | 40.059 | | | | |
| 13177.7 | 6880.7 | E | 9.518 | | | | |
| 15898.1 | 10174.8 | | | | | | |
| 17615.4 | 11063.2 | D and E values are given in cm ⁻¹ | | | | | |
| 18021.0 | 11303.3 | | | | | | |
| 20414.8 | 12028.4 | | | | | | |
| 20561.3 | 13340.5 | | | | | | |
| 21610.9 | 13497.6 | | | | | | |
| 21723.9 | 16064.1 | | | | | | |
| 22982.1 | 17703.5 | | | | | | |
| 23411.4 | 18251.6 | | | | | | |
| 24017.7 | 20527.6 | | | | | | |
| 25997.1 | 20799.3 | | | | | | |
| 27895.9 | 21574.0 | | | | | | |
| 28544.4 | 21882.8 | | | | | | |
| 29435.2 | 22036.2 | | | | | | |
| 30303.4 | 23082.4 | | | | | | |
| 30735.9 | 23517.0 | | | | | | |
| 32020.2 | 23660.0 | | | | | | |
| 32939.2 | 24380.5 | | | | | | |
| 33365.1 | 26226.2 | | | | | | |
| 34043.3 | 28053.7 | | | | | | |
| 35558.6 | 28073.9 | | | | | | |
| 36832.5 | 28717.3 | | | | | | |
| 37337.1 | 29567.2 | | | | | | |
| 37733.2 | 30460.4 | | | | | | |
| 39807.6 | 31036.0 | | | | | | |
| 39965.4 | 32990.8 | | | | | | |
| 42253.8 | 33104.3 | | | | | | |
| 43129.1 | 33681.7 | | | | | | |
| 43510.6 | 34400.7 | | | | | | |
| 47920.5 | 35748.5 | | | | | | |
| 48640.9 | 36964.1 | | | | | | |
| 48923.6 | 37544.1 | | | | | | |
| 51839.6 | 37931.9 | | | | | | |
| 52210.1 | 40032.4 | | | | | | |
| 52548.5 | 40212.1 | | | | | | |
| 53183.3 | 42484.7 | | | | | | |
| 67706.6 | 43323.1 | | | | | | |
| 71995.5 | 43791.7 | | | | | | |
| 74157.0 | 47954.1 | | | | | | |
| 76016.5 | 48929.7 | | | | | | |
| 77817.9 | 49198.6 | | | | | | |

Table S7. MOLCAS CASSCF+RASSI computed spin-free and spin-orbit state energies for complex 1.

| Spin-free energies (cm ⁻¹) | Spin-orbit states (cm ⁻¹) | CASSCF+RASSI computed results | | | | | |
|----------------------------------------|---------------------------------------|------------------------------------------------|---------|----------------|---------|----------|----------|
| 0.0 | 0.0 | g _X | 2.039 | X _M | 0.82005 | 0.03743 | -0.57107 |
| 1638.3 | 0.0 | g _Y | 2.290 | Y _M | 0.07639 | 0.98177 | 0.17404 |
| 3129.4 | 83.8 | g _Z | 2.558 | Z _M | 0.56718 | -0.18635 | 0.80224 |
| 6849.5 | 1744.3 | | | | | | |
| 11055.2 | 1840.8 | D _X | 25.811 | X _A | 0.87989 | 0.01392 | -0.47497 |
| 13356.6 | 3141.0 | D _Y | -3.642 | Y _A | 0.10285 | 0.97030 | 0.21897 |
| 21837.0 | 3296.7 | D _Z | -22.168 | Z _A | 0.46391 | -0.24152 | 0.85232 |
| 23732.7 | 4522.7 | D | 38.716 | | | | |
| 28358.0 | 6989.3 | E | 9.263 | | | | |
| 33409.0 | 7077.6 | | | | | | |
| 4200.4 | 10258.2 | D and E values are given in cm ⁻¹ | | | | | |
| 10306.9 | 11218.6 | | | | | | |
| 11939.7 | 11432.0 | | | | | | |
| 16335.2 | 12064.9 | | | | | | |
| 17767.8 | 13515.2 | | | | | | |
| 18038.5 | 13652.4 | | | | | | |
| 20745.9 | 16492.0 | | | | | | |
| 20951.0 | 17844.2 | | | | | | |
| 21706.7 | 18279.7 | | | | | | |
| 23111.0 | 20850.9 | | | | | | |
| 24107.7 | 21179.0 | | | | | | |
| 26459.0 | 21688.9 | | | | | | |
| 28792.4 | 21998.0 | | | | | | |
| 29567.3 | 22136.9 | | | | | | |
| 30300.8 | 23242.9 | | | | | | |
| 30825.6 | 23759.4 | | | | | | |
| 32164.5 | 23958.5 | | | | | | |
| 33385.6 | 24520.2 | | | | | | |
| 34024.6 | 26677.0 | | | | | | |
| 35604.1 | 28501.6 | | | | | | |
| 37108.0 | 28525.5 | | | | | | |
| 37703.6 | 28961.6 | | | | | | |
| 38096.2 | 29699.3 | | | | | | |
| 40119.7 | 30482.5 | | | | | | |
| 40245.6 | 31109.9 | | | | | | |
| 42670.0 | 32325.0 | | | | | | |
| 43615.4 | 33318.3 | | | | | | |
| 43987.2 | 33518.9 | | | | | | |
| 48047.8 | 33825.6 | | | | | | |
| 48599.1 | 34423.3 | | | | | | |
| 48946.6 | 35791.0 | | | | | | |
| 51825.6 | 37239.1 | | | | | | |
| 52290.4 | 37906.5 | | | | | | |
| 52627.6 | 38288.8 | | | | | | |
| 53252.1 | 40329.1 | | | | | | |
| 66951.8 | 40491.9 | | | | | | |
| 71460.8 | 42897.9 | | | | | | |
| 73553.3 | 43802.3 | | | | | | |
| 75501.6 | 44255.7 | | | | | | |
| 77358.6 | 48059.0 | | | | | | |

Table S8. ORCA CASSCF computed spin-free and spin-orbit state energies for complex **2**.

| Spin-free energies (cm ⁻¹) | Spin-orbit states (cm ⁻¹) | CASSCF computed results | | | | | |
|----------------------------------------|---------------------------------------|------------------------------------------------|---------|----------------|---------|----------|----------|
| | | | | | | | |
| 0.0 | 0.0 | g _X | 2.027 | X _M | 0.92192 | -0.09222 | -0.37625 |
| 1559.9 | 82.9 | g _Y | 2.284 | Y _M | 0.08442 | 0.99574 | -0.03722 |
| 2865.4 | 1665.1 | g _Z | 2.551 | Z _M | 0.37808 | 0.00255 | 0.92577 |
| 4142.0 | 1765.8 | | | | | | |
| 6494.4 | 2903.5 | D _X | 7.401 | X _A | 0.95887 | -0.10740 | -0.26275 |
| 10289.4 | 3044.6 | D _Y | -10.839 | Y _A | 0.10221 | 0.99420 | -0.03339 |
| 10744.0 | 4444.6 | D _Z | 36.588 | Z _A | 0.26481 | 0.00516 | 0.96429 |
| 12134.7 | 6642.1 | D | 38.307 | | | | |
| 13125.1 | 6726.2 | E | 9.120 | | | | |
| 15717.5 | 10192.7 | | | | | | |
| 17582.6 | 10910.1 | D and E values are given in cm ⁻¹ | | | | | |
| 18103.4 | 11185.2 | | | | | | |
| 20167.6 | 12200.0 | | | | | | |
| 20467.7 | 13285.0 | | | | | | |
| 21532.9 | 13461.2 | | | | | | |
| 21549.7 | 15884.1 | | | | | | |
| 22823.1 | 17675.8 | | | | | | |
| 23394.3 | 18318.3 | | | | | | |
| 23824.5 | 20300.3 | | | | | | |
| 25766.8 | 20691.4 | | | | | | |
| 27293.4 | 21478.2 | | | | | | |
| 28400.2 | 21706.1 | | | | | | |
| 29286.4 | 21883.1 | | | | | | |
| 30315.2 | 22943.0 | | | | | | |
| 30539.3 | 23425.7 | | | | | | |
| 31996.7 | 23625.3 | | | | | | |
| 32377.0 | 24224.3 | | | | | | |
| 33154.8 | 25995.3 | | | | | | |
| 34038.6 | 27458.5 | | | | | | |
| 35339.5 | 27477.9 | | | | | | |
| 36635.1 | 28570.9 | | | | | | |
| 36985.8 | 29409.6 | | | | | | |
| 37374.4 | 30432.2 | | | | | | |
| 39559.2 | 30858.0 | | | | | | |
| 39774.1 | 32485.3 | | | | | | |
| 41894.9 | 32576.2 | | | | | | |
| 42782.6 | 33447.3 | | | | | | |
| 43066.9 | 34338.0 | | | | | | |
| 47452.3 | 35523.4 | | | | | | |
| 48220.7 | 36752.5 | | | | | | |
| 48626.1 | 37190.1 | | | | | | |
| 51357.5 | 37573.0 | | | | | | |
| 51691.0 | 39781.9 | | | | | | |
| 52045.6 | 40013.3 | | | | | | |
| 52666.5 | 42120.6 | | | | | | |
| 67606.0 | 42957.5 | | | | | | |
| 71676.4 | 43362.8 | | | | | | |
| 73744.3 | 47489.1 | | | | | | |
| 75382.1 | 48519.9 | | | | | | |
| 77189.1 | 48878.0 | | | | | | |

Table S9. MOLCAS CASSCF+RASSI computed spin-free and spin-orbit state energies for complex **2**.

| Spin-free energies (cm ⁻¹) | Spin-orbit states (cm ⁻¹) | CASSCF+RASSI computed results | | | | | |
|----------------------------------------|---------------------------------------|------------------------------------------------|---------|-------|----------|----------|---------|
| | | | | | | | |
| 0.0 | 0.0 | g_X | 2.041 | X_M | -0.82828 | -0.03317 | 0.55934 |
| 1635.2 | 79.9 | g_Y | 2.303 | Y_M | 0.05614 | 0.98831 | 0.14176 |
| 2989.8 | 1737.8 | g_Z | 2.555 | Z_M | 0.55750 | -0.14882 | 0.81673 |
| 6704.3 | 1836.5 | | | | | | |
| 10892.9 | 3037.1 | D_X | -21.125 | X_A | -0.87709 | -0.02151 | 0.47984 |
| 13258.3 | 3163.1 | D_Y | -3.485 | Y_A | 0.08496 | 0.97630 | 0.19906 |
| 21590.4 | 4713.9 | D_Z | 24.610 | Z_A | 0.47275 | -0.21536 | 0.85448 |
| 23697.3 | 6847.0 | D | 36.915 | | | | |
| 27708.4 | 6931.0 | E | 8.820 | | | | |
| 32807.7 | 10342.0 | | | | | | |
| 4438.2 | 11054.7 | D and E values are given in cm ⁻¹ | | | | | |
| 10438.4 | 11320.6 | | | | | | |
| 12205.1 | 12284.1 | | | | | | |
| 16176.7 | 13414.9 | | | | | | |
| 17758.9 | 13575.4 | | | | | | |
| 18148.0 | 16334.4 | | | | | | |
| 20530.2 | 17842.5 | | | | | | |
| 20863.0 | 18369.6 | | | | | | |
| 21644.4 | 20650.3 | | | | | | |
| 22955.7 | 21078.8 | | | | | | |
| 23913.1 | 21574.8 | | | | | | |
| 26240.1 | 21751.2 | | | | | | |
| 28654.4 | 21945.2 | | | | | | |
| 29422.0 | 23091.8 | | | | | | |
| 30304.9 | 23647.2 | | | | | | |
| 30639.2 | 23911.0 | | | | | | |
| 32141.3 | 24374.7 | | | | | | |
| 33188.0 | 26457.1 | | | | | | |
| 34003.0 | 27862.5 | | | | | | |
| 35340.1 | 27882.0 | | | | | | |
| 36847.8 | 28819.8 | | | | | | |
| 37291.9 | 29544.7 | | | | | | |
| 37680.4 | 30460.5 | | | | | | |
| 39811.6 | 30925.7 | | | | | | |
| 40009.4 | 32294.1 | | | | | | |
| 42272.1 | 32857.6 | | | | | | |
| 43213.5 | 32982.6 | | | | | | |
| 43497.0 | 33512.4 | | | | | | |
| 47558.4 | 34313.5 | | | | | | |
| 48128.0 | 35520.7 | | | | | | |
| 48577.0 | 36965.7 | | | | | | |
| 51304.9 | 37491.0 | | | | | | |
| 51725.0 | 37871.9 | | | | | | |
| 52077.4 | 40022.4 | | | | | | |
| 52690.7 | 40243.4 | | | | | | |
| 66815.3 | 42494.6 | | | | | | |
| 71083.1 | 43383.1 | | | | | | |
| 73085.2 | 43776.7 | | | | | | |
| 74815.6 | 47564.7 | | | | | | |
| 76676.3 | 48437.0 | | | | | | |

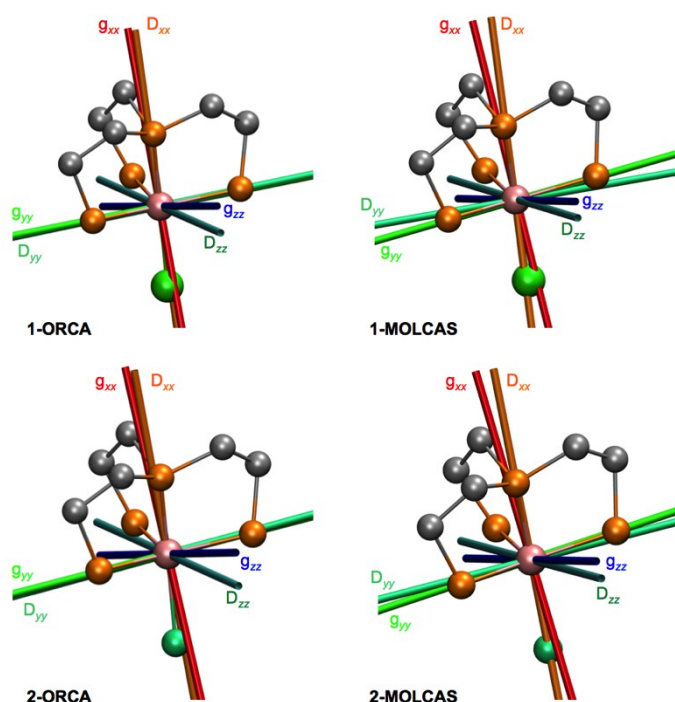


Fig. S6. Orientation of the computed g - and D -tensors for complexes **1** and **2** with ORCA and MOLCAS.

Additional discussion about the comparison between the studied complexes with the ones reported in the literature

We have carried out an exploration of the CSD looking for other Co^{II} complexes containing P_4 ligands (either mono or polydentate) and one halide, which could be compared to complexes **1** and **2** (Table 2, entries 1-7). For those complexes we have carried out a CASSCF calculation equivalent to those of **1** and **2**, and we have also computed their SHAPE analysis respect the typical 5 vertex polyhedra. Among the complexes found, 3 are trigonal bipyramids (DIZQAF, NIZDOP and UFUCUV), 3 correspond to vacant octahedron structures (JIPCER01, VAKFAR and VAKFEV) and the last one (RUTSUU) seems to be in between of the spherical square pyramid and the trigonal bipyramid shapes (although closer to the latter). The computed D values are positive regardless the shape or the nature of the ligands forming the complexes; the only exception is DIZQAF, which has a negative D value probably because the E/D parameter is close to the acceptable 0.3 limit value. There are other parameters derived from the calculations that indicate DIZQAF should have a positive D value. For instance, the composition of the Kramer's doublets (KD) of this structure indicates that the $m_s = \pm 1/2$ terms dominate the first KD while the $m_s = \pm 3/2$ terms are more important in the second one. This qualitatively indicates that the D value should be positive. In addition, shows that the d-orbital ordering obtained with the AILF is (from lower to higher energies): d_{xz} , d_{yz} , d_{xy} , $d_{x^2-y^2}$ and d_{z^2} , indicating the first transition should happen between the d_{xz} (or d_{yz}) and d_{xy} orbitals; since these orbitals have a different $|m_l|$ value, the contribution to the D value should be positive. This is also observed by checking the composition of the low energy determinants for this complex.

The question is: can we compare these $\text{Co}^{\text{II}}\text{-P}_4\text{X}_1$ complexes **1** and **2** to the corresponding nitrogenated $\text{Co}^{\text{II}}\text{-N}_4\text{X}_1$ analogous structures? The answer is no, and this is because there is not any equivalent structures present in both sets. The most similar N_4X_1 structure we have found corresponds to the CSD code

FAWYUX (Fig. S7 and Table 2, entry 8). This complex has a neutral tetradentate N-ligand and a chloride as substituents for the cobalt center, in a square pyramid arrangement where one of the nitrogen atoms takes the axial position (as does P in complexes **1** and **2**). The E/D ratio for this complex is also quite high (0.28) and raises questions about the true nature of the sign of D . However, the computed parameters ascertain that D should be positive for this complex. As above, the $m_s = \pm 1/2$ terms dominate the first KD while the $m_s = \pm 3/2$ terms are stronger in the second KD, indicative of a qualitatively positive D value. In this case the AILF method indicates that the d-orbital ordering is (from lower to higher energies): d_{xz} , d_{yz} , d_{xy} , d_{z^2} and $d_{x^2-y^2}$, stating that the first transition should happen between the d_{xz} (or d_{yz}) and d_{xy} orbitals; hence producing a positive D . This is also confirmed by the composition of the low energy determinants for this complex. Of course, there are other N_4X_1 structures displaying a square pyramidal structure and those have been also computed as the ones above (Table 2, entries 9-12). As may be observed the computed D values take both signs but only those with an E/D ratio lower than 0.3 should be trusted (NADTUH and NUQMAP). On the other hand, RUJSOE and XOBFEZ, have negative D values and an E/D ratio higher than 0.3 and thus other computed features (as shown above) have to be trusted for defining the sign of D . In both cases the $m_s = \pm 1/2$ terms dominate the first KD while the $m_s = \pm 3/2$ terms are higher in the second KD. The d-orbital ordering obtained with the AILF is (from lower to higher energies): d_{xz} , d_{yz} , d_{xy} , $d_{x^2-y^2}$ and d_{z^2} for both complexes. This indicates that the first transition should happen between the d_{xz} (or d_{yz}) and d_{xy} orbitals; since these orbitals have a different $|m_l|$ value, the contribution to the D value should be positive.

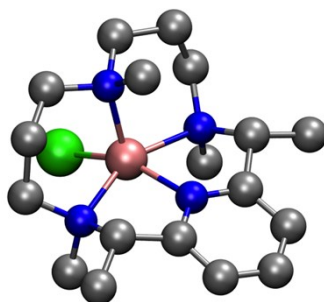


Fig. S7. Structure of the Co(II)- N_4X_1 complex FAWYUX. Color code: Co = pink, C = gray, N = blue, Cl = green, all H atoms have been omitted.

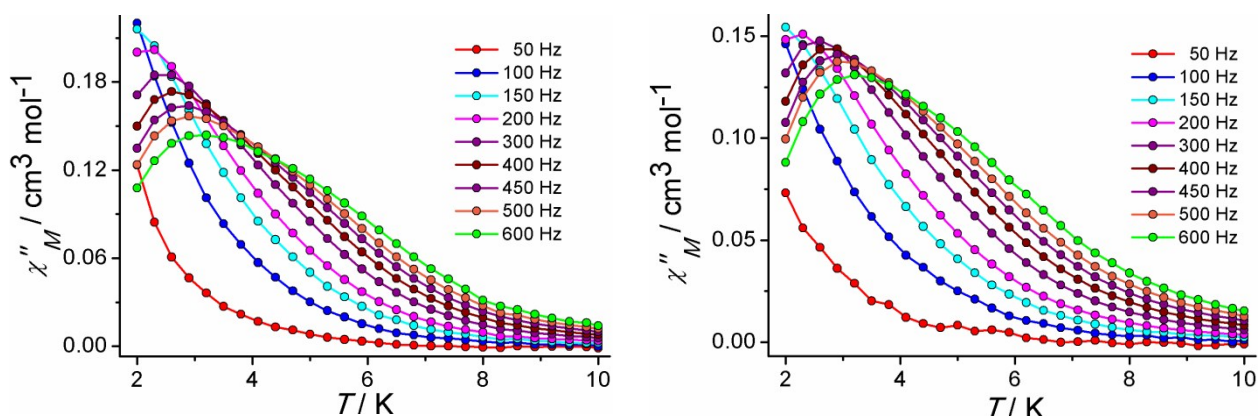


Fig. S8. Temperature dependency of the out-of phase (χ_M'') ac magnetic susceptibility plots for complex **1** (left) and **2** (right) under 1000 Oe dc field.

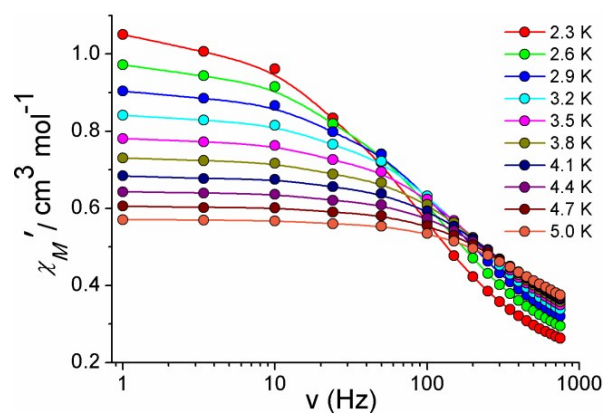


Fig. S9. Frequency dependency of the in-phase ac susceptibility plots for complex **1** under 1000 Oe dc field.

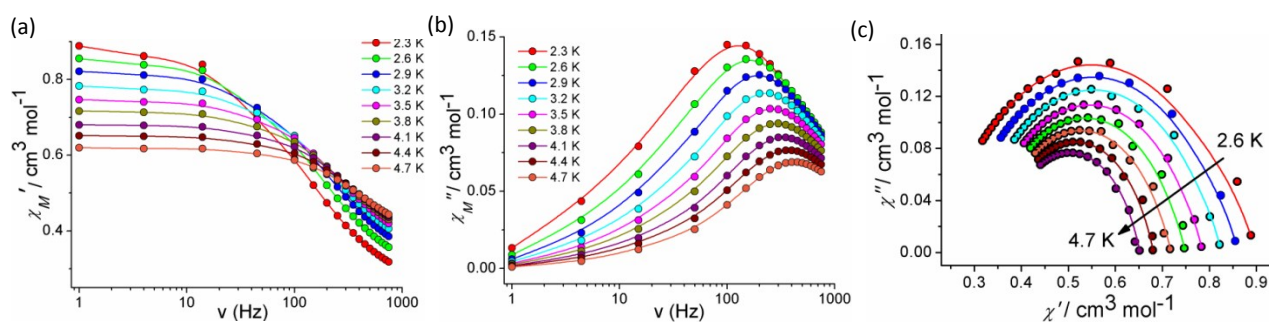


Fig. S10. Frequency dependency of the in-phase (a) and out-of phase (b) ac susceptibility plots for complex **2** under 1000 Oe dc field. Cole-Cole plots for complex **2** (c). Solid lines represent the best fit.

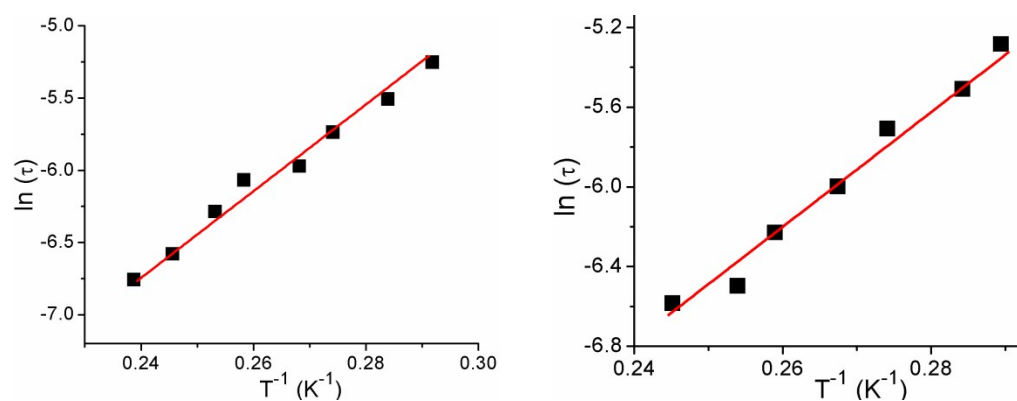


Fig. S11. $\ln(\tau)$ vs. $1/T$ plot for complex **1** (left) and **2** (right). The red line is the best fit of the Arrhenius relationship.

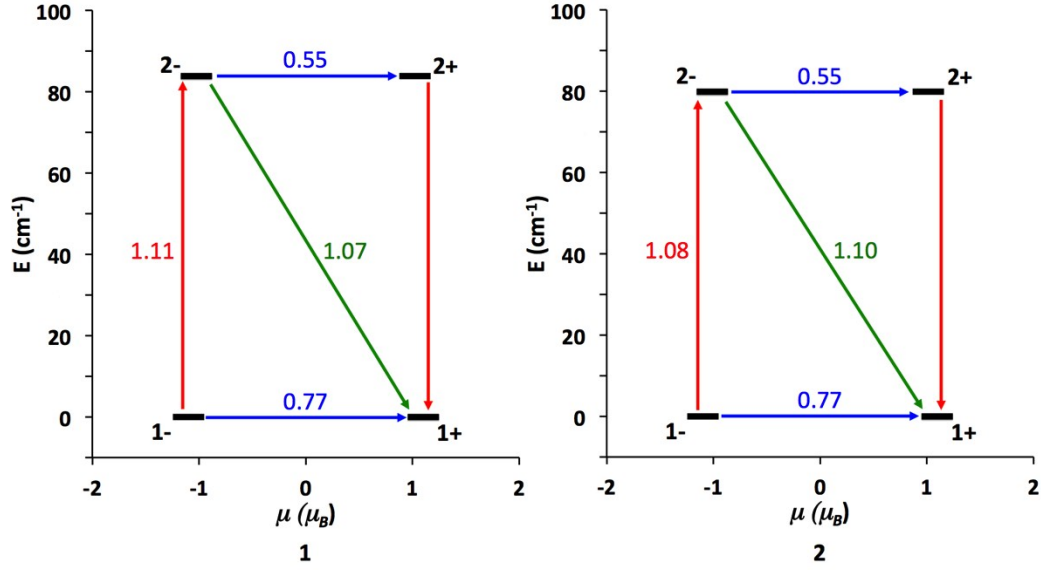


Fig. S12 Lowest two Kramer's doublets and *ab initio* computed relaxation mechanism in **1** (left) and **2** (right). The thick black lines imply KDs as a function of their magnetic moment along the main anisotropy axis. Red lines indicate the magnetization reversal mechanism. The blue lines correspond to ground state QTM and thermally assisted-QTM via the first excited KD, and green lines show possible Orbach relaxation processes. The values close to the arrows indicate the matrix elements of the transition magnetic moments (above 0.1 an efficient spin relaxation mechanism is expected).

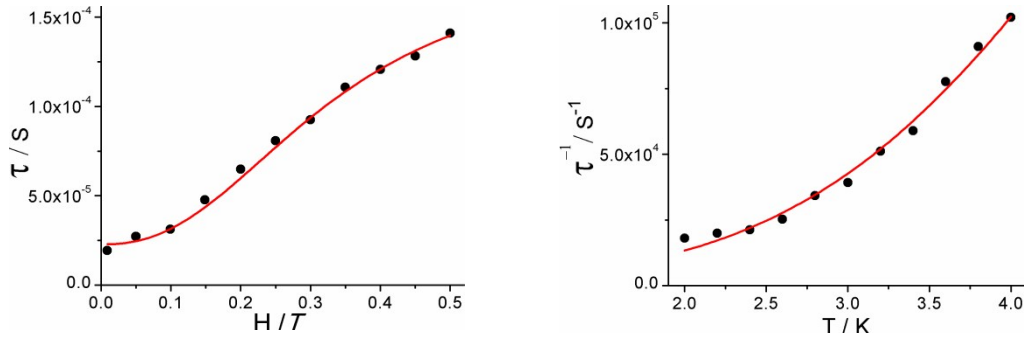


Fig. S13. Field dependency of the average relaxation time for **1** at 2 K (left). τ^{-1} vs temperature for **1** at 0.1 T dc field (right). The red lines are the best fits obtained according to equations 3 and 4 respectively, described in the main text.

References:

1. G. M. Sheldrick, *SHELXTL Program for the Solution of Crystal of Structures*, University of Göttingen, Göttingen, Germany, 1993.
2. G. M. Sheldrick, *SHELXL 97, Program for Crystal Structure Refinement*, University of Göttingen, Göttingen, Germany, 1997.

3. A. L. Spek, *J Appl. Crystallogr.*, 2003, **36**, 7-13.
4. L. J. Farrugia, *J. Appl. Crystallogr.*, 1999, **32**, 837-838.
5. O. Kahn, *Molecular Magnetism*, VCH Publishers Inc., New York, USA, 1991.
6. (a) G. Karlström, R. Lindh, P.-Å. Malmqvist, B. O. Roos, U. Ryde, V. Veryazov, P.-O. Widmark, M. Cossi, B. Schimmelpfennig, P. Neogrady and L. Seijo, *Comput. Matter Sci.*, 2003, **28**, 222-239; (b) V. Veryazov, P.-O. Widmark, L. Serrano-Andrés, R. Lindh and B. O. Roos, *Int. J. Quantum Chem.*, 2004, **100**, 626-635; (c) F. Aquilante, L. De Vico, N. Ferré, G. Ghigo, P.-Å. Malmqvist, P. Neogrady, T. B. Pedersen, M. Pitoňák, M. Reiher, B. O. Roos, L. Serrano-Andrés, M. Urban, V. Veryazov and R. Lindh, *J. Comp. Chem.*, 2010, **31**, 224-247.
7. F. Neese, *WIREs Comput. Mol. Sci.*, 2012, **2**, 73-78.
8. (a) L. F. Chibotaru, L. Ungur and A. Soncini, *Angew. Chem. Int. Ed.*, 2008, **47**, 4126-4129; (b) L. F. Chibotaru, L. Ungur, C. Aronica, H. Elmoll, G. Pillet and D. Luneau, *J. Am. Chem. Soc.*, 2008, **130**, 12445.
9. (a) B. O. Roos, V. Veryazov and P.-O. Widmark, *Theor. Chim. Acta.*, 2004, **111**, 345; (b) B. O. Roos, R. Lindh, P.-Å. Malmqvist, V. Veryazov and P.-O. Widmark, *J. Phys. Chem. A*, 2004, **108**, 2851; (c) B. O. Roos, R. Lindh, P.-Å. Malmqvist, V. Veryazov and P.-O. Widmark, *J. Phys. Chem. A*, 2005, **109**, 6575-6579; (d) B. O. Roos, R. Lindh, P.-Å. Malmqvist, V. Veryazov and P.-O. Widmark, *Chem. Phys. Letters*, 2005, **409**, 295-299.
10. (a) F. Weigend and R. Ahlrichs, *Phys. Chem. Chem. Phys.*, 2005, **7**, 32997-33305; (b) F. Weigend, *Phys. Chem. Chem. Phys.*, 2006, **8**, 1057-1065.